ELSEVIER

Earth and Planetary Science Letters 171 (1999) 575–589

EPSL

www.elsevier.com/locate/epsl

First seamount age evidence for significantly slower African plate motion since 19 to 30 Ma

J.M. O'Connor [a,*], P. Stoffers [a], P. van den Bogaard [b], M. McWilliams [c]

[a] *Institute for Geosciences, Christian-Albrechts-University, D-24118 Kiel, Germany*
[b] *GEOMAR Research Center, Wischhofstrasse 1–3, D-24148 Kiel, Germany*
[c] *Department of Geophysics, Stanford University, Stanford, CA 94305-2215, USA*

Received 8 March 1999; revised version received 21 July 1999; accepted 22 July 1999

Abstract

Resolving the time–space (and compositional) evolution of volcanism along long-lived South Atlantic hotspot trails is important to understanding the connection between hotspot volcanism and mantle plumes. $^{40}Ar/^{39}Ar$ ages are reported here for rocks dredged from a line of five individual seamounts along an ~290 km northeast to southwest line extending from the vicinity of Saint Helena Island, and also for Circe Seamount. These seamounts were created in a midplate setting and could have formed rapidly (≤1 Myr). The St. Helena Seamount ages reveal a remarkably linear migration rate of volcanism of 20 ± 1 mm/yr for at least the past 19 Myr, which is interpreted as the absolute motion of the African plate. Because this is much slower than estimated for earlier African plate migration it also represents the first evidence based on seamount ages for a significant deceleration (~33%) of the African plate since at least 19 Ma. However, this change could have occurred as early as 30 Ma when the limited data for the Tristan/Gough hotspot chain are also considered. This deceleration supports a relationship between African plate speed and the upsurge of hotspot volcanism on the African continent at ~25 Ma. We suggest that the increased number of oceanic African hotspots between ~19 and 30 Ma points to a link also between major changes in plate motion and the onset and continuation of oceanic hotspot volcanism. Our study supports the assumption that chains of individual, rapidly (?) formed seamounts have considerably more potential of providing clear insights into how mantle plumes interact with overriding lithosphere than do those consisting of uninterrupted, more massive lines of hotspot volcanism.

Keywords: Africa; absolute age; hotspot; Ar-40/Ar-39; plume; Atlantic Ocean

1. Introduction

Establishing the geological history of trails of South Atlantic hotspot volcanism is of much importance to eventually understanding the processes controlling the development of mantle plumes, generally considered to be responsible for the creation of such volcanism [1]. Many studies investigate the influence of mantle plumes on the compositional variability of the Mid-Atlantic Ridge (MAR) (e.g., [2–7]). Such studies provide information about the relatively recent influence of S. Atlantic mantle plumes on oceanic lithosphere. Another approach is to investigate the time–space and compositional history of volcanism along long-lived hotspot chains. In the

* Corresponding author. Present address: Alfred Wegener Institute for Polar and Marine Research, Columbusstrasse, D-27515 Bremerhaven, Germany. Fax: +49 471 4831 149; E-mail: joconnor@awi-bremerhaven.de

0012-821X/99/$ – see front matter
PII: S0012-821X(99)00183-1

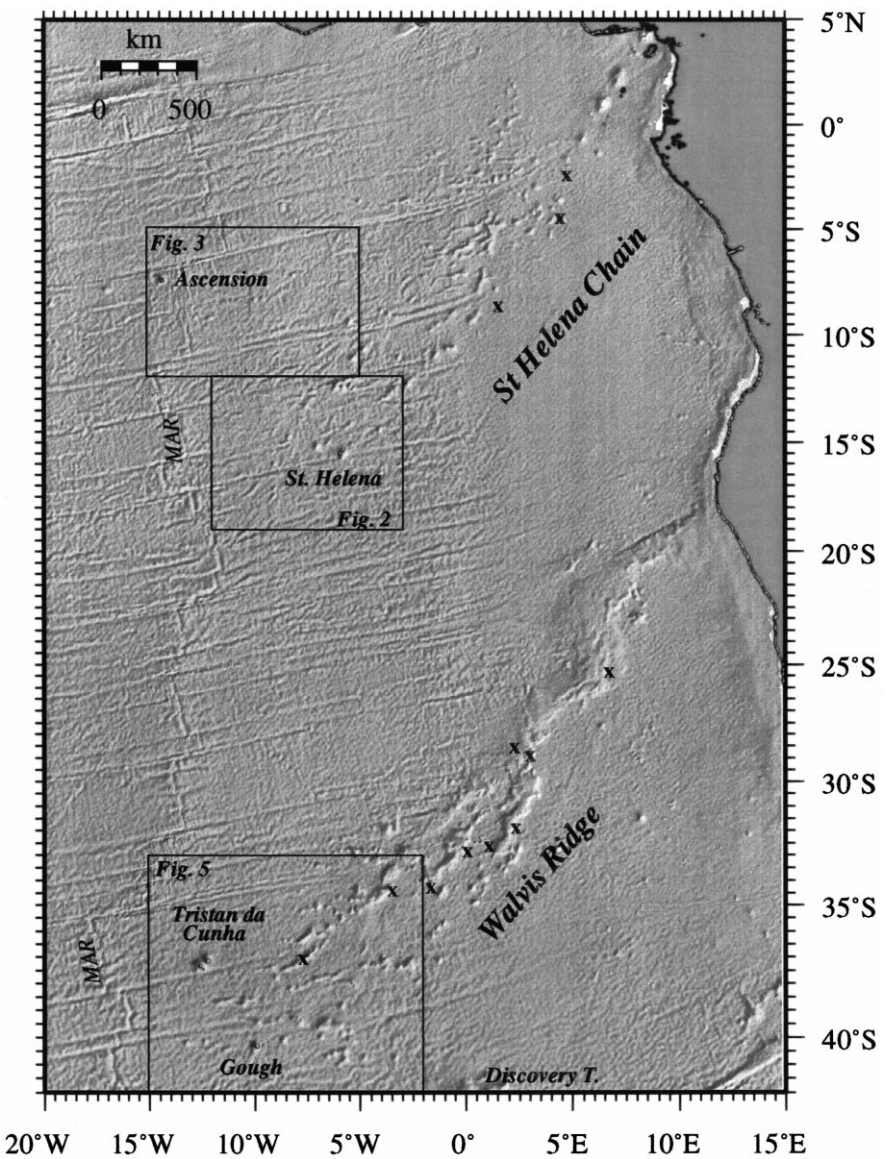

Fig. 1. Predicted topography of the Eastern S. Atlantic [15]. Dredge sites for which $^{40}Ar/^{39}Ar$ ages have been published previously are indicated by an X [11,12]. *Discovery T.* = Discovery Tablemount. *MAR* = Mid-Atlantic Ridge.

case of the S. Atlantic only two such chains have been generated by mantle plumes since the opening of the S. Atlantic — the volcanic trails of the St. Helena and Tristan/Gough hotspots [8–14] (Fig. 1). The influence of these mantle plumes, which are very distinct in Sr–Nd–Pb isotopic arrays [16], on the MAR has been demonstrated [2–4,6,7,17]. Furthermore, the St. Helena Seamount Chain (Fig. 1) was shown via the spatial distribution of $^{40}Ar/^{39}Ar$-dated seamounts to have been created as a result of African plate motion over a hotspot located in the vicinity of St. Helena Island [12]. Similarly, age data demonstrated that the Walvis Ridge (Fig. 1) is the product of African plate migration over a hotspot located in the region of the islands of Tristan da Cunha and Gough [11,12]. Although these studies led to the

first order conclusion that the St. Helena and Walvis hotspot trails formed by the drift of the African plate over mantle plumes, the $^{40}Ar/^{39}Ar$ data base is still too small to reliably estimate migration rates of volcanism, and so by inference, the history of African plate motion. Therefore, a better understanding of the time–space (and compositional) histories of these trails can provide important information about the following unresolved issues:

(a) The regional distribution of St. Helena and Tristan/Gough hotspot volcanism through time.

(b) Identify and quantify changes in the absolute motion of the African plate.

(c) Determine whether the upsurge in hotspot volcanism on the African continent (previously attributed to the African plate coming to a halt at ~25 Ma and remaining virtually motionless since [18]) can be correlated with a change in African absolute plate motion.

(d) The extent to which the St. Helena and Tristan/Gough plumes have remained stationary since the opening of the S. Atlantic.

Prior to this study the youngest known midplate volcanism associated with the St. Helena hotspot was the last phase of volcanism on St. Helena Island between 7 and 8 Myr [19–21]. The F.S. *Sonne* was used therefore to search for evidence of active hotspots at the SW end of the St. Helena Chain (Fig. 2) and also at Circe Seamount (Fig. 3) [24]. Circe Seamount is located ~900 km to the north of the SW end of the St. Helena Chain and has been proposed as the site of an active hotspot [2].

We report here high precision $^{40}Ar/^{39}Ar$ ages for rocks dredged from Circe Seamount and from along an ~290 km line of six individual seamounts extending SW from Bagration Seamount (located ~57 km NW of St. Helena Island) (Fig. 2). These ages indicate rapid seamount formation ($\leq$1 Myr) and show that volcanism has migrated linearly at a rate of 20 ± 1 mm/yr between Bagration (18 to 19 Ma) and Josephine seamounts (2.6 Ma) (Fig. 2). Because this is significantly slower than estimates for the earlier history of the St. Helena Chain, we conclude that the absolute motion of the African plate has been ~33% slower since at least 19 Ma (and possibly as early as 30 Ma when age data for the Tristan/Gough hotspot trail are taken into consideration). This is the first evidence based on the distribution of dated seamounts for such a slowdown.

Our results support an earlier suggestion of a

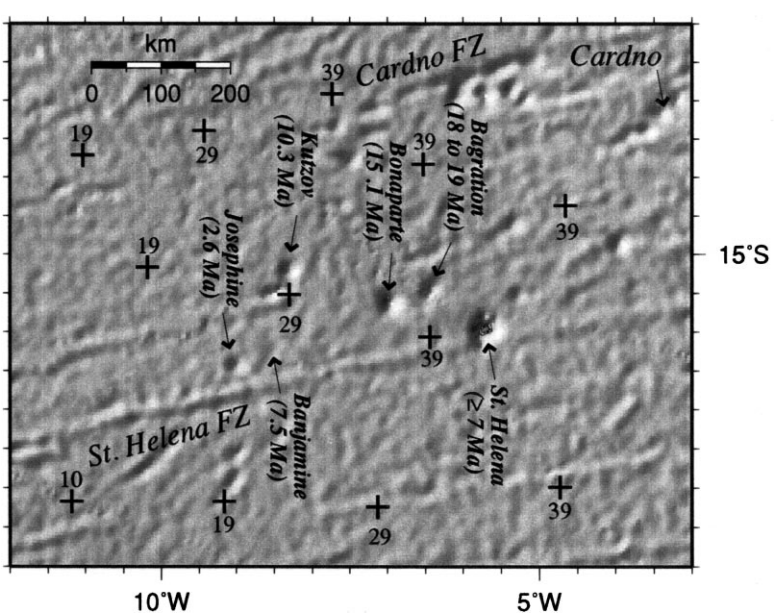

Fig. 2. Predicted topography of the SW St. Helena Seamount Chain [15]. Seamount ages shown are from this study. Plus (+) symbols indicate seafloor magnetic anomalies [22] and their assigned ages (young side of anomalies) are after the time scale of [23]. Age estimate for St. Helena Island is from [21].

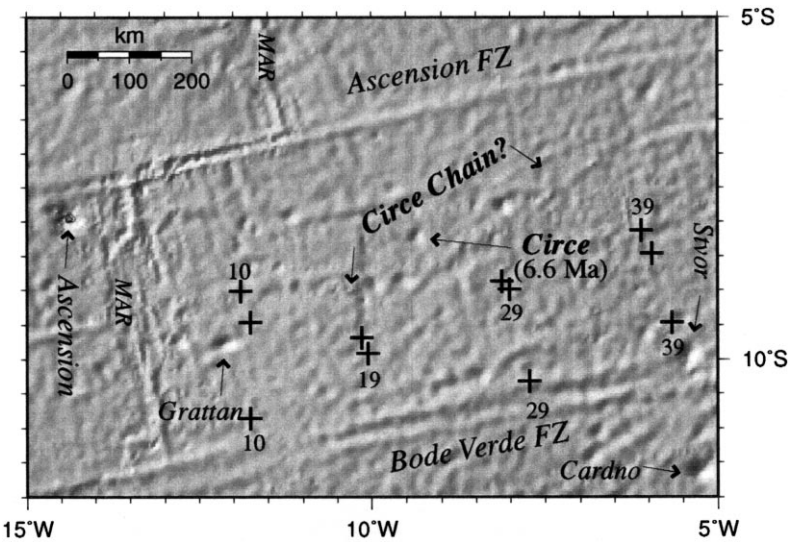

Fig. 3. Predicted topography of the Circe Seamount region [15]. Shown are the location and the age reported here for Circe Seamount and the possible Circe Seamount Chain (between arrows). Other details as in Fig. 2.

causal relationship between African plate motion and an upsurge of hotspot volcanism on the African continent [18]. We speculate here that evidence exists also for a relationship between changes in African plate motion and an increase in oceanic hotspot volcanism. Furthermore, our study provides supporting evidence for the recent finding, based on SE Pacific studies [25], that age dating of individual, rapidly (?) formed seamounts has much greater potential of providing clearer insights into how mantle plumes interact with overriding lithosphere than more massive uninterrupted chains of volcanism, e.g., the Walvis Ridge or Hawaiian Chain. Such an approach could therefore finally resolve, for example, the much debated question of hotspot fixity and other related questions.

2. Sample preparation and analytical procedure

Bonaparte Seamount sample M16/1 was recovered during a cruise of the F.S. *Meteor* [26] and was analyzed at Stanford University, USA. The remainder, recovered during a cruise of the F.S. *Sonne* [24], were analyzed using the laser probe system at the Geomar Research Center, Kiel. $^{40}Ar/^{39}Ar$ single fusion ages for two of these samples were measured also by laser probe at the Vrije University, Amsterdam. Descriptions and locations of dredge samples are in Table 1.

Pieces of selected rock samples, following removal with a saw of outer surfaces and as much visible alteration as possible, were crushed and sieved. Altered whole rock samples (500–250 μm) were treated with 7 N HCl prior to treatment for 1 hour in 1 N HNO_3 (in an ultrasonic bath at 50ºC) followed by rinsing in distilled water. Plagioclase (250 and 125 μm) was separated from crushed whole rock using a magnetic separator and first treated in 7 N HCl for 30 min, then in 5–8% HF for 5 min, followed by 1 hour in 1 N HNO_3. The samples were then washed in distilled H_2O. Extensive alteration and addition of alteration products sometimes required the repetition of certain steps.

Plagioclase and whole rock chip samples were placed in 99.9% pure aluminum foil packets, each of which was secured in one of a series of custom-drilled holes in a 99.95% pure aluminum disk. Sample disks, interspersed with a 3-dimensional array of 27.92 Ma TCR (85G003) sanidine monitor [27], were secured together and then sealed in an aluminum can and irradiated with Cd shielding at the Geesthacht Research Center (Germany). Samples were shielded by a 0.5 mm Cd liner during the 72 hour irradiation at 5 MW (in Position 44) with a fast neutron fluence of 2.1×10^{12} N cm^{-2}

Table 1
Sample information

Sample	Seamount	Location on bottom off bottom	Depth (m) on bottom off bottom	Description
SO84 7DS-1	Circe	8°12.545′S 9°19.819′W 8°12.588′S 9°19.613′W	2126 2085	Small piece of vesicular, fine-grained basalt, 2 mm Mn-crust, alteration veins
SO84 43DS-1	Kutzov	15°08.400′S 8°21.131′W 15°08.710′S 8°21.173′W	1990 1966	Highly altered, vesicular phyric lava with plag phenos (to 20 mm)
SO84 53DS-1	Benjamin	16°11.918′S 8°30.951′W 16°12.128′S 8°30.817′W	2640 2299	Altered aphyric vesicular lava
SO84 60DS-2	Josephine	16°22.999′S 9°00.665′W 16°23.119′S 9°00.305′W	1785 1605	Moderately vesicular and altered basalt, microphenos of plag
SO84 68DS-1	Bonaparte	15°36.270′S 7°06.846′W 15°36.140′S 7°05.718′W	3300 3019	Altered vesicular lava with rare plag phenos (to 5 mm)
SO84 68DS-2	Bonaparte	15°36.270′S 7°06.846′W 15°36.140′S 7°05.718′W	3300 3019	Altered lava with large vesicles taken from conglomerate with many lava pieces
SO84 68DS-5	Bonaparte	15°36.270′S 7°06.846′W 15°36.140′S 7°05.718′W	3300 3019	Altered lava with trachytic texture taken from same conglomerate as 68DS-2
SO84 68DS-6	Bonaparte	15°36.270′S 7°06.846′W 15°36.140′S 7°05.718′W	3300 3019	Altered, vesicular, phyric lava with large plag phenos (to 10 mm), taken from same conglomerate as 68DS-2 and 68DS-5
SO84 69DS-2	Bonaparte	15°48.410′S 6°57.229′W 15°47.947′S 6°56.072′W	2987 2791	Altered, vesicular, phyric lava with large plag phenos (to 10 mm)
M16/1-6[a]	Bonaparte	15°38.5′S 7°00.7′W	1268	Altered, vesicular and phyric lava with large plag phenos (to 10 mm)
SO84 71DS-6	Bagration	15°22.768′S 6°33.596′W 15°23.195′S 6°32.689′W	4112 3467	Altered, aphyric and vesicular pillow piece with large plag phenos (to 10 mm)
SO84 72DS-2	Bagration	15°24.886′S 6°29.493′W 15°25.102′S 6°28.955′W	3092 2876	Altered, vesicular and phyric pillow lava with plag phenos (to 10 mm)
SO84 73DS-1	Bagration	15°25.331′S 6°28.533′W 15°25.901′S 6°28.361′W	2641 2553	Highly altered, vesicular lava piece with some small phenos of plag
SO84 74DS-1	Bagration	15°26.597′S 6°27.947′W 15°26.909′S 6°27.808′W	2248	Altered, vesicular and phyric lava with plag phenos (to 10 mm)

[a] Measured at Stanford University.

s^{-1}. TCR standard was measured between 3 and 4 times for each monitor position (4 levels with 8 positions = 32 positions). The appropriate J-value and associated error was interpolated for each sample position using a 3-dimensional least-squares cosine plane fit [C. Hall, pers. commun.] For each interpolated J-value the uncertainty was $<0.1\%$. The maximum horizontal variation across the disk stack was $<2\%$, and the maximum vertical variation was 6.3%. $^{40}Ar/^{39}Ar$ laser analyses were conducted at the Geomar Tephrochronology Laboratory using a 25 W Spectra Physics argon ion laser and a MAP 216 series mass spectrometer fitted with a Baur-Signer ion source and a Johnson electron multiplier. Raw mass spectrometer peaks were corrected for mass discrimination, background values (determined between every one or two analyses), and interfering neutron reactions on Ca and K using CaF_2 and K_2SO_4 salts that had been irradiated together with the samples.

The theory of $^{40}Ar/^{39}Ar$ geochronology is described in [28–30]. Sample ages were calculated using the standard age equation. The uncertainty in the age was calculated by partial differentiation of the age equation [31] and includes uncertainties in the determination of the flux monitor, J, the blank determination, the regression of the intensities of the individual isotopes, the correction factors for interfering isotopes, and the mass discrimination correction. Data reduction involved standard procedures, i.e., the error calculations used the error estimates of each of the Ar isotopes derived from the scatter about the regression to zero (inlet) time, then propagated these errors back to the age and the isotope ratio estimates based on a complete set of partial derivatives, considering the perturbations in the measured values of the Ar isotopes. Errors included also those from monitors and blank runs, and are quoted at the 1σ level.

Ages and error estimates were calculated for each sample discussed here by calculating the mean apparent age (single fusion ages weighted by the inverse of their variance; [32]) of each population, assuming an initial 'atmospheric' $^{40}Ar/^{39}Ar$ ratio of 295.5. Isochrons have been calculated as inverse isochrons using York's least squares fit that accommodates errors in both ratios and correlation of errors [33]. Mean squared weighted deviates (MSWD) were determined for the mean apparent ages in order to test the scatter of the single fusion data (e.g., [34]). These data sets represent isochrons, i.e., the MSWD is low (often $\sim$1 and always $<$2.5) and the isochron ages overlap with the mean apparent ages (within analytical uncertainty). In cases where the scatter around the plateaus or isochrons is greater than predicted from the analytical errors, i.e., MSWD $>$ 1, the analytical error has been expanded by multiplying by the $\sqrt{\text{MSWD}}$ (e.g., [33]).

Plagioclase from Bonaparte Seamount dredge sample M16/1 was dated both by incremental heating in a resistance furnace at Stanford University (see [35] for analytical procedure) and by multiple laser fusions at Geomar, Kiel. The fact that these results agree within analytical uncertainty (discussed in the following section) demonstrates the reliability of our data. In addition, two single fusion ages measured using a laser probe at the Vrije University, Amsterdam, support our results for Benjamin and Josephine Seamounts (see [25,36] for analytical procedure). Intercalibration between the Stanford and Vrije University $^{40}Ar/^{39}Ar$ systems showed that there is no systematic bias in the handling of data [36].

3. Results

The primary argon isotopic data are in **EPSL Online Background Dataset 1** [1]. $^{40}Ar/^{39}Ar$ age calculations are summarized in Table 2. Plateau and inverse isochron plots are in **Online Background Dataset 2** [1]. Following is a discussion of the results for each individual seamount (Figs. 2 and 3).

3.1. Bagration Seamount

Ages were determined for rock samples dredged from four stations located along the NW flank between approximately 4100 and 2100 m water depth. Samples from the two deeper dredges were similar in age (weighted average of 17.9 ± 0.3 Ma) as also were those from the two shallower dredges (weighted average of 18.8 ± 0.2 Ma) (Table 3).

3.2. Bonaparte Seamount

Dredge samples from stations located on (1) the NW flank at $\sim$3000 m (i.e., both in situ and conglomerate rocks), (2) upslope of this site at $\sim$1270 m and (3) the SE flank at a depth of $\sim$2800 m all gave the same age (within analytical uncertainty). The weighted average of all measured ages was 15.05 ± 0.03 Ma, inclusive of the incremental heating resistance furnace result from Stanford University (Table 3). The 15.1 ± 0.5 Ma resistance furnace age for sample M16/1-6 agreed with the multiple laser fusion age for the same sample (15.1 ± 0.2 Ma) and again also with the weighted average of all multiple laser fusion ages (15.1 ± 0.03 Ma) (Table 3).

3.3. Kutzov Seamount

An age of 10.3 ± 0.3 Ma was measured for a single sample from a dredge station located on the NW flank at a depth of $\sim$2000 m.

[1] http://www.elsevier.nl/locate/epsl, mirror site: http://www.elsevier.com/locate/epsl

Table 2
Age calculations from Argon isotopic data

Sample	Seamount	Mean age (Ma)	±1σ	MSWD	Isochron age (Ma)	±1σ	MSWD	Initial	±1σ	N used	Material
SO84 7DS-1	Circe	6.6	0.1	1.1	6.6	0.1	1.1	295	2	18	whole rock
SO84 43DS-1	Kutzov	10.1	0.3	1.9	10.3	0.3	1.7	294	1	13	plagioclase
SO84 53DS-1	Benjamin	7.8	0.3	0.7	7.5	0.5	0.7	295.9	0.4	15	plagioclase
SO84 53DS-1 [a]	Benjamin				7.30	0.03					
SO84 60DS-2	Josephine	2.5	0.2	0.1	2.6	0.3	0.1	283	13	7	plagioclase
SO84 60DS-2 [a]	Josephine				2.80	0.04					
SO84 71DS-6	Bagration	17.8	0.3	0.4	17.9	0.3	0.5	294	4	6	plagioclase
SO84 72DS-2	Bagration	18.6	0.4	0.9	18.0	0.5	0.7	299	1	8	plagioclase
SO84 73DS-1	Bagration	18.9	0.2	1.3	18.8	0.2	1.2	299	2	10	plagioclase
SO84 74DS-1	Bagration	18.9	0.2	0.4	18.9	0.3	0.5	296	1	8	plagioclase
SO84 68DS-1	Bonaparte	15.7	0.5	2.2	15.3	1.1	2.5	297	4	7	plagioclase
SO84 68DS-2	Bonaparte	15.10	0.03	1.6	15.10	0.03	1.1	309	5	12	plagioclase
SO84 68DS-5	Bonaparte	15.00	0.03	0.6	14.9	0.1	0.6	298	2	8	plagioclase
SO84 68DS-6	Bonaparte	15.3	0.4	2.0	14.2	0.6	1.5	298	1	15	plagioclase
SO84 69DS-2	Bonaparte	15.3	0.5	1.6	14.5	0.5	1	298	1	11	plagioclase
M16/1-6	Bonaparte	15.1	0.1	0.7	15.1	0.2	0.7	297	16	11	plagioclase
		Weighted plateau age									
M16/1-1 [b]	Bonaparte	15.4	0.2		15.1	0.5	0.8	307	15	7	plagioclase

[a] Vrije University (Netherlands) laser single fusion data.
[b] Stanford University (USA) resistance furnace incremental heating data.

3.4. Benjamin Seamount

A single dredge sample from a station located on the northern side was shown to be 7.5 ± 0.5 Ma. This result was supported by a single fusion age of 7.30 ± 0.03 Ma measured at the Vrije University Amsterdam.

3.5. Josephine Seamount

A sample from a single dredge station located on the northern side at ~1600 m was 2.6 ± 0.3 Ma. This result was supported by a single fusion age of 2.80 ± 0.04 Ma also measured at the Vrije University Amsterdam.

3.6. Circe Seamount

A sample from a dredge station located on the NW flank was determined to be 6.6 ± 0.1 Ma.

4. Discussion

4.1. Duration of volcanism on individual seamounts

Our age data suggest the possibility that individual seamounts along the St. Helena Chain formed rapidly (Table 2). In the case of Bagration Seamount the age difference between the two deeper and two shallower dredge stations, which represent a systematic sampling of a complete seamount flank, indicates that it formed in as little as 1 Myr. A series of dredge stations on Bonaparte Seamount at various depths and locations all show a uniform age of formation (within analytical uncertainty). The fact that these ages have been measured on samples from dredge stations widely distributed across the seamount (and include conglomerate rocks) also supports the rapid formation of this, and also by inference, other St. Helena Chain seamounts. As there is only a single age measurement in the cases of Kutzov, Benjamin and Josephine Seamounts, we cannot establish the rate at which they formed.

Table 3
Individual seamount ages

	Mean age	$\pm1\sigma$	Isochron age	$\pm1\sigma$
	Bonaparte Seamount			
	15.7	0.5	15.3	1.1
	15.10	0.03	15.10	0.03
	15.00	0.03	14.9	0.1
	15.3	0.4	14.2	0.6
	15.3	0.5	14.5	0.5
	15.1	0.1	15.1	0.2
GEOMAR data: Weighted average	15.07	0.02	15.05	0.03
Stanford U. incremental heating data	15.4	0.2	15.1	0.5
Combined data: Weighted average	15.08	0.02	15.05	0.03
	Bagration Seamount (older phase)			
	17.8	0.3	17.9	0.3
	18.6	0.4	18	0.5
Weighted average	18.1	0.2	17.9	0.3
	Bagration Seamount (younger phase)			
	18.9	0.2	18.8	0.2
	18.9	0.2	18.9	0.3
Weighted average	18.9	0.1	18.8	0.2
	Bagration Seamount (all age data)			
	17.8	0.3	17.9	0.3
	18.6	0.4	18	0.5
	18.9	0.2	18.8	0.2
	18.9	0.2	18.9	0.3
Weighted average	18.7	0.1	18.6	0.1

4.2. Migration rate of volcanism along the St. Helena Chain

Dated seamounts at the SW end of St. Helena Chain (Fig. 2) have a remarkably linear trend of decreasing age showing that volcanism has migrated along the SW-orientated Bagration (18–19 Ma) to Josephine (2.6 Ma) seamount chain at a rate of 20 ± 1 mm/yr (Fig. 4a). When this rate is considered in combination with that estimated from the very few published ages for the older part of the St. Helena Chain (Fig. 1), it becomes apparent that the migration rate of volcanism along the chain has been significantly slower (~33%) since at least 19 Ma (Fig. 4b,c). Also, comparison of seamount and seafloor ages (Fig. 2) shows that the St. Helena seamounts discussed here all formed in a midplate tectonic setting. Due to the lack of seafloor ages in the region it is only possible to estimate the age of seafloor at the time of seamount loading at between 20 and 16 Ma (Fig. 2).

The linear migration of volcanism to the SW from Bagration Seamount suggests that — despite the fact that subaerial volcanic activity occurred as recently as 7 to 8 Ma ago on St. Helena Island [19–21] — its submarine core could be significantly older, i.e., similar in age to the 18–19 Myr old Bagration Seamount located only ~57 km to the NW.

4.3. Circe Seamount

An active Circe hotspot has been identified on the basis of co-latitudinal spreading-axis geochemical and bathymetric anomalies with Circe Seamount (Fig. 3) being proposed as its present location [2]. Our $^{40}Ar/^{39}Ar$ age of 6.6 ± 0.1 Ma for a dredged rock sample shows that, although Circe Seamount formed in a midplate setting (on 19 to 29 Myr seafloor at the time of seamount creation) (Fig. 3), i.e., has a hotspot origin, it is no longer associated with an active hotspot. However, we speculate that because of Circe Seamount's midplate origin it could

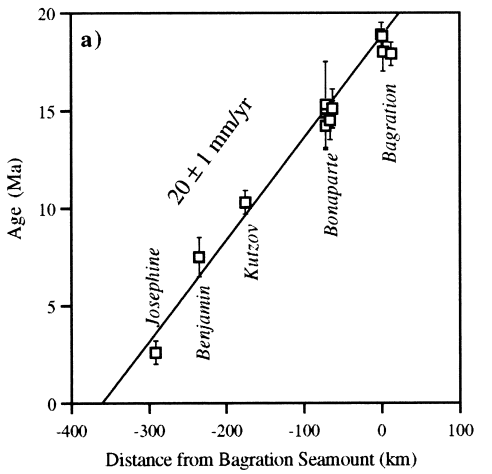

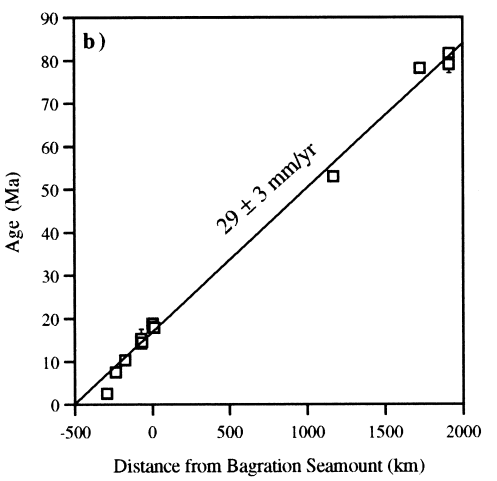

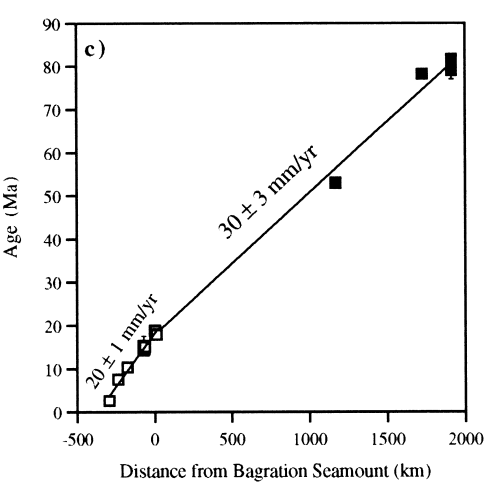

Fig. 4. (a) Migration rate of volcanism between Bagration and Josephine Seamounts (York-2 regression [33], not forced through the origin). As Kutzov Seamount is offset to the north of the Bagration to Josephine line (Fig. 2), its location was projected orthogonally onto this lineament. However, omitting the age for Kutzov when regressing the data did not change the estimated migration rate. 2σ error bars for measured ages are evident whenever larger than symbols. (b) Migration rate of volcanism along the entire St. Helena Chain estimated on the basis of all available $^{40}Ar/^{39}Ar$ age data (simple linear regression, not forced through the origin). Ages from this study and [12]. Other details as in (a). (c) Younger and older $^{40}Ar/^{39}Ar$ ages were regressed separately (York-2 and simple linear regression, respectively). Regression of the older age data was forced through the 18–19 Ma ages for Bagration Seamount due to a lack of available ages. Other details as in (a).

be part of a hotspot trail, i.e., the indistinct short band of scattered seamounts trending towards a region of the MAR (Fig. 3) that is being influenced by a mantle plume [2–4,7,37]. If correct, this points to the existence of an active hotspot about 130 km SW of Circe Seamount (Fig. 3) on the basis of local plate velocity calculated for the St. Helena Chain (Fig. 4).

4.4. Slowdown of the African plate

Following [1], the linear migration rate of midplate volcanism along the northeast to southwest trending Bagration to Josephine line of seamounts can be interpreted as record of local linear absolute velocity of the African plate in a hotspot reference frame. Therefore, our preferred explanation for the apparent change in the migration rate of volcanism along the St. Helena Chain (Fig. 4) is that the absolute motion of the African plate has been about 33% slower since at least 19 Ma. One explanation for this slowdown could be collision with the Eurasian plate beginning about 38 Ma (e.g., [38]). Although no active midplate volcanism associated with the St. Helena hotspot is known, we show that hotspot volcanism as young as 2.6 Ma exists ~290 km to the SW of St. Helena Island.

4.5. Migration rate of volcanism along the Tristan/Gough hotspot trail

The only other hotspot trail in the S. Atlantic with a long-lived history comparable to that of the St. Helena Chain has been produced by a hotspot

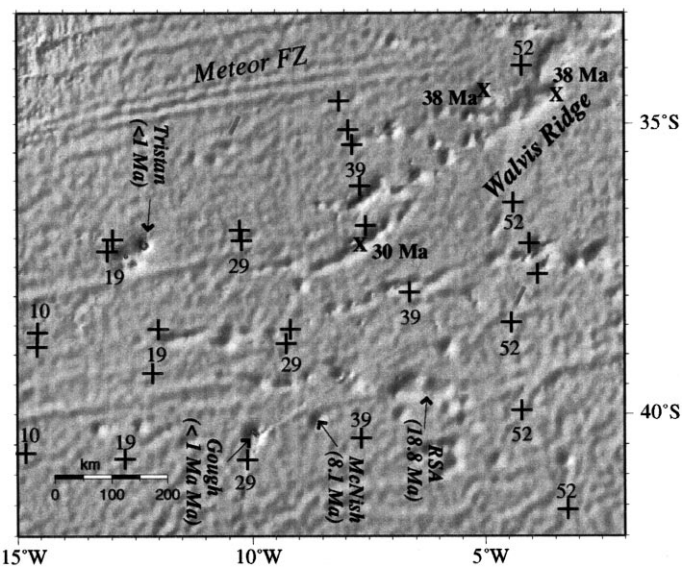

Fig. 5. Predicted topography of the region around the islands of Tristan da Cunha and Gough and the SW end of the Walvis Ridge [15]. Seamount ages are from [11,12]. Age estimate for Gough Island is from [39,12] and for Tristan da Cunha from [40,12]. Other details as in Fig. 2.

located in the region of the islands of Tristan da Cunha and Gough (Figs. 1 and 5). The SW end of this trail consists of an ~400 km-wide region of scattered seamounts, small ridges and islands (Fig. 5), basically similar in morphology to that of the St. Helena Chain (Fig. 2). Because of the relatively few seamount ages reported for the Tristan/Gough region [11,12], it is not possible to reconstruct migration rates of volcanism as reliably (Fig. 6) as in the case of the SW end of St. Helena Chain (Fig. 4). Nonetheless, a migration rate of 22 ± 2 mm/yr (Fig. 6a) was determined across the southern boundary of this region. This line of seamounts is similar in orientation to that of the Bagration to Josephine Chain. The relative difference between the calculated migration rates of volcanism (i.e., local linear plate velocities) of the St. Helena and Tristan/Gough trails (20 ± 1 and 22 ± 2 mm/yr, respectively) is reasonable in terms of what would be expected from changing linear plate velocity with increasing distance from likely Euler poles for reconstructing African absolute plate motion since 30 Ma.

Confirming that a change in African plate motion occurred at ~19 Ma is not possible due the relatively few age data, especially in view of their generally very high analytical uncertainties (Fig. 6). Estimating any relative motion between the St. Helena and Tristan/Gough hotspots is therefore also not feasible. Nonetheless, our best estimate based on available age data from along the Tristan/Gough trails is that the change in African plate speed occurred at ~30 Ma. This leads us to bracket the timing of proposed African deceleration, on the basis of available age data for both the St. Helena and Tristan/Gough trails, at between 19 and 30 Ma.

4.6. Implications of a slower African plate

Increased cordilleran activity along the western edge of the S. American plate beginning between 25 and 30 Ma [42] has been explained by acceleration of the South American plate [43] in response to a slowdown of the African plate [38]. This appears to be supported by the data presented here.

An upsurge in hotspot volcanism on continental Africa beginning at ~25 Ma and continuing to the present day has been attributed to a motionless African plate [18]. Our results contribute to this debate by indicating that, although the African plate has not been stationary, a causal relationship could exist between hotpot volcanism on the African continent and a significant (~33%) slowdown of the

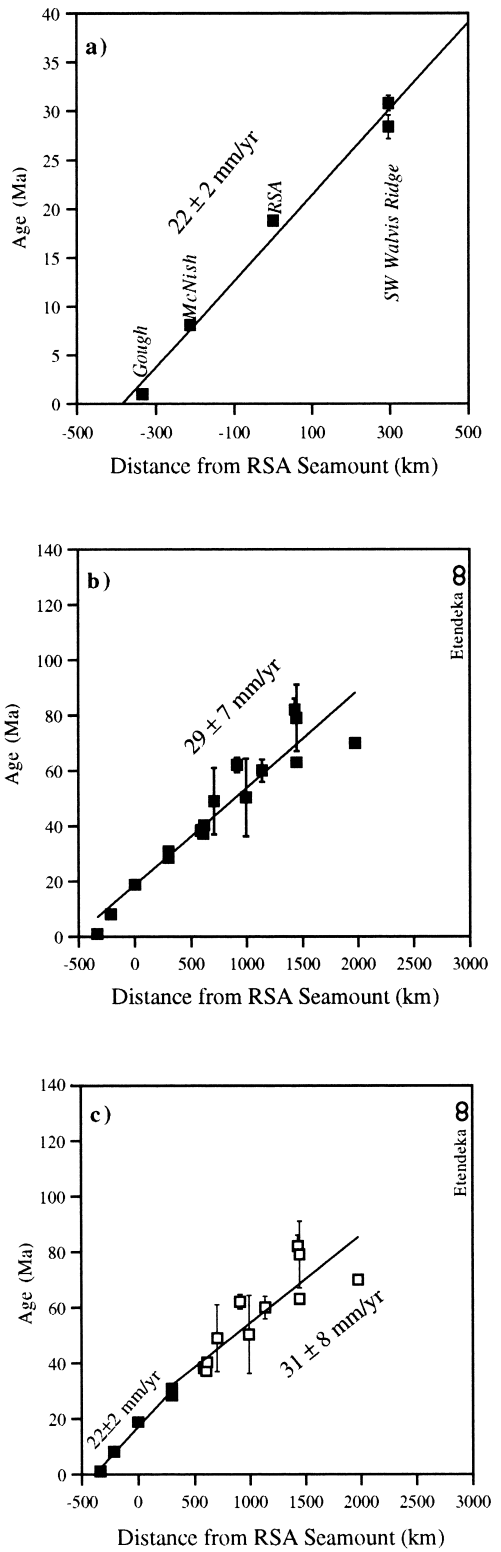

African plate. Because of the much greater complexity of continental geology, it is not surprising that such a motion change has apparently first been detected in an oceanic setting. Therefore, it seems that continued studies of a possible link between continental hotspot volcanism on the African plate and changing plate motion should combine oceanic and continental approaches.

We propose that the apparent onset of volcanism between ~20 and 30 Ma associated with a number of African oceanic hotspots, and its continuation since, is evidence for the influence of plate motion on the behavior of hotspots also on the oceanic part of the African plate. For example, ages of shield phases within the Canary Islands show that volcanism has migrated westward since about 20 Ma from Fuerteventura Island [44]. However, shield ages are not well constrained for most of these islands, with volcanism continuing to the present day on many. In the case of the Cape Verdes, a number of studies have been made of the onset of volcanic activity and, although they come to different conclusions as to the time of onset, they all agree that there has been intense volcanic activity since 20 Ma (e.g., [45]). The oldest part of the Discovery hotspot chain, located to the South of the Tristan–Gough Chain (Fig. 1), would appear to have been formed at about 25 Ma, based on a K–Ar age for Discovery Tablemount [46]. The creation of the proposed Circe Seamount Chain (Fig. 3), could have been initiated by African plate deceleration. Increased oceanic hotspot volcanism proposed here may also have influenced hotspot/spreading axis interactions. A new map of spreading asymmetries in the South

Fig. 6. (a) The migration rate of volcanism between the SW Walvis Ridge and Gough Island (York-2 regression [33], not forced through the origin) (Fig. 5). 2σ error bars for measured ages are evident whenever larger than symbols. Other details as in Fig. 5. (b) Migration rate of volcanism along the Gough Island–RSA seamount–Walvis Ridge lineament estimated on the basis of all available $^{40}Ar/^{39}Ar$ age data (simple linear regression, not forced through the origin). Etendeka continental flood basalt age range (not included in data regression) is from [41]. Other details as in (a) or Fig. 5. (c) Younger and older $^{40}Ar/^{39}Ar$ age data were regressed separately (York-2 and simple linear regression, respectively). Regression of the younger ages includes those from the SW Walvis Ridge, as does that of the older age data. Other details as in (a) and (b).

Atlantic ([47], their Fig. 1b) shows that asymmetries in the spreading corridors close to St. Helena increased since chron 13 (~33 Ma), and in the case of Tristan da Cunha, also became more pronounced between chrons 13 and 6 (~20 Ma). This observation corresponds very well with an increase in hotspot volcanism linked to changing African absolute plate motion. It also agrees with the conclusion [47] that ridge–hotspot interaction, as expressed in ridge jumps/propagations towards a hotspot, is more dependent on the magnitude/volume of hotspot volcanism than on the distance between the ridge and the hotspot.

One possible explanation for changes in the behavior of African hotspots is an interplay between changing lithospheric stress (e.g., [48,49]) (in response to the deceleration of the African plate) and enhanced heating of the lithosphere due to slower plate motion over hotter regions in the mantle, i.e., upwelling mantle plumes. Changing lithospheric stresses due to plate deceleration could have triggered the onset of hotspot volcanism in new areas located over hot areas of the mantle (e.g., [48,25]). However, this would require that mantle plumes are upwelling in many more locations, or under wider regions of the sub-lithosphere, without producing evidence in the form of hotspot trails (e.g., [13,50]), than is presently indicated by the 'classic' mantle plume hypothesis [1].

4.7. Deciphering plate motion from chains of scattered seamounts

The question arises as to whether bands of individual seamounts such as the St. Helena Seamount Chain can be explained simply in terms of linear migration rates of volcanism that record plate motion over a stationary plume. By far the most extensive $^{40}Ar/^{39}Ar$ study of a seamount chain similar in morphology to that of St. Helena is the $\geq$1900 km long, $\geq$21 Myr old Foundation Seamount Chain, SE Pacific [25]. These seamounts apparently formed relatively rapidly, i.e. in $\leq$1 Myr, as is also being proposed here for the St. Helena, and by inference, for the SW Tristan/Gough trails. The Foundation Chain ages convincingly demonstrate that not only do such bands of isolated seamounts record absolute plate speed, but do so very reliably [25]. This conclusion is supported by the predicted migration rate of volcanism along the Hawaiian Chain.

However, in order to conclusively confirm and quantify plate motion changes for the African plate, a sufficient number of samples from seamounts across the St. Helena and Tristan/Gough hotspot trails need to be dated. Although local intraplate stress and/or preexisting lithospheric weaknesses have possibly played a role in the formation of the SW end of the St. Helena and Tristan/Gough chains, we feel that the linear progression of their ages points to this being a minor factor. This conclusion is supported by the results of the Foundation Seamount Chain study where the influence of such localized factors on the distribution of hotspot volcanism was clearly distinguishable from the overall linear trend on the basis of anomalous ages [25].

5. Conclusions

Isolated seamounts at the younger end of the St. Helena Chain ($\leq$19 Ma) possibly formed rapidly ($\leq$1 Myr) as indicated by ages of rocks dredged from several locations on both Bagration and Bonaparte Seamounts. This supports a similar conclusion based on a study of the Foundation Seamount Chain, SE Pacific [25], which has a morphology similar to that of the St. Helena Chain.

Comparison of seamount and seafloor ages shows that the seamounts dated in this study all formed in a midplate tectonic setting, i.e., on seafloor that ranged between ~20 and 16 Ma at the time of seamount creation.

Volcanism has migrated at a rate of 20 ± 1 mm/yr in a SW direction along the St. Helena Chain since at least 19 Ma, based on the distribution of the $^{40}Ar/^{39}Ar$ dated seamounts, which is interpreted as an absolute motion of the African plate.

St. Helena Island may have started forming as early as 19 Ma based on the age of the nearby Bagration Seamount, and the linear migration rate of volcanism along the St. Helena Chain. This would indicate that the island had a volcanic history of possibly 12 Myr.

From the distribution of all dated St. Helena seamounts it is apparent that a significant decrease (~33%) in the migration rate of volcanism had oc-

curred along the St. Helena Chain by 19 Ma. This is in turn interpreted as reflecting a slowdown of the African plate, which is supported to some extent by current estimates of the migration rates of volcanism along the volcanic trail of the Tristan/Gough hotspot. However, the combined information from the St. Helena and Tristan/Gough trails can only bracket the time of plate motion change to between 19 to 30 Ma.

Circe Seamount is shown not to be the site of the active Circe hotspot, as previously proposed. However, its creation in a midplate setting indicates that it is related to a hotspot (most likely Circe?). Based on the estimates given here for African plate speed for the past $\geq$19 Ma, an active Circe hotspot could exist 130 km to the SW of Circe Seamount.

The hypothesis that a major upsurge in hotspot volcanism on the African continent at $\sim$25 Ma was due to a motionless African plate [18] requires modification in light of our evidence for African plate slowdown. In addition, we suggest that a change in hotspot behavior also occurred on the oceanic part of the African plate (e.g., Canaries, Cape Verdes, Discovery and possibly Circe hotspots). A recent study of the asymmetry of crustal accretion in the South Atlantic [47] further supports this conclusion.

We present the first clear evidence based on the distribution of dated seamounts for significantly slower African plate motion since at least 19 Ma and possibly as early as 30 Ma. The fact that bands of rapidly formed (?), scattered and isolated S. Atlantic seamounts successfully record plate motion (as previously shown for Foundation Chain seamounts, SE Pacific) has significant implications for future sampling of oceanic hotspot trails in order to reconstruct plate motion, determine whether hotspots are stationary and define the mechanisms controlling plume–lithosphere interaction. The suggestion that the onset of new oceanic regions of African hotspot volcanism, and their continued activity, might be influenced by changes in plate motion over a mantle, may represent a valuable link between hotspot volcanism and mantle plumes.

Acknowledgements

Captain H. Papenhagen, officers and crew are thanked for their excellent handling of the F.S. *Sonne*. They are also thanked, along with D. Ackermand, for successfully dredging the rock samples used in this study. G. Wefer and C.W. Devey supplied sample M16/1. J. Geldmacher assisted with post cruise sample preparations. J. Sticklus provided technical support during $^{40}Ar/^{39}Ar$ laser dating at Geomar. J.R. Wijbrans generously provided laser dating facilities to JO'C at the Vrije University, Amsterdam. JO'C thanks M. Lanphere and J. Saburomaru, U.S.G.S. for advice on sample preparation and B. Hacker for advice while working on sample M16/1 at Stanford University. W. Weinrebe provided gray shaded predicted topography maps. The SO84 cruise of the F.S. *Sonne* was funded by Bundesministerium für Forschung und Technologie project 527618-029618 (P. Stoffers). This study was supported by Deutsche Forschungsgemeinschaft project Sto 110/25-1 (P. Stoffers). We thank D. Müller, J. Wijbrans, and an anonymous reviewer for their very thoughtful reviews that have led to significant improvements. ***[RV]***

References

[1] W.J. Morgan, Convection plumes in the lower mantle, Nature 230 (1971) 42–43.
[2] J.-G. Schilling, G. Thompson, R. Kingsley, S. Humphris, Hotspot-migrating ridge interaction in the South Atlantic, Nature 313 (1985) 187–191.
[3] B.B. Hanan, R.H. Kingsley, J.-G. Schilling, Pb isotope evidence in the South Atlantic for migrating ridge–hotspot interactions, Nature 322 (1986) 137–144.
[4] D.W. Graham, W.J. Jenkins, J.-G. Schilling, G. Thompson, M.D. Kurz, S.E. Humphris, Evidence from geoid data of a hotspot origin for the southern Mascarene Plateau and Mascarene helium isotope geochemistry of mid-ocean ridge basalts from the South Atlantic, Earth Planet. Sci. Lett. 110 (1992) 133–147.
[5] J.-G. Schilling, B.B. Hanan, B. McCully, R.H. Kingsley, D. Fontignie, Influence of the Sierra Leone Mantle plume on the equatorial Mid-Atlantic Ridge: A Nd–Sr–Pb isotopic study, J. Geophys. Res. 99 (1994) 12005–12028.
[6] J. Douglass, J.-G. Schilling, R.H. Kingsley, C. Small, Influence of the Discovery and Shona mantle plumes on the southern Mid-Atlantic Ridge: Rare earth evidence, J. Geophys. Res. 22 (1995) 2893–2896.
[7] D. Fontignie, J.-G. Schilling, Mantle heterogeneities beneath the South Atlantic: a Nd–Sr–Pb isotope study along the Mid-Atlantic Ridge (3°S–46°S), Earth Planet. Sci. Lett. 142 (1996) 209–221.
[8] W.J. Morgan, Plate motions and deep mantle convection,

Geol. Soc. Am., Mem. 132 (1972) 1–7.
[9] W.J. Morgan, Hot-spot tracks and the opening of the Atlantic and Indian Oceans, in: The Sea, Wiley Interscience, New York, 1981, pp. 443–488.
[10] R.A. Duncan, Hotspots in the Southern Oceans. An absolute frame of reference of motion of the Gondwana continents, Tectonophysics 74 (1981) 29–42.
[11] J.M. O'Connor, R.A. Duncan, Evolution of the Walvis Ridge–Rio Grande Rise hot spot-system: Implications for African and South American plate motions over plumes, J. Geophys. Res. 95 (1990) 17475–17502.
[12] J.M. O'Connor, A.P. le Roex, South Atlantic hot spot–plume systems: 1. Distribution of volcanism in time and space, Earth Planet. Sci. Lett. 113 (1992) 343–364.
[13] L. Fleitout, C. Dalloubeix, C. Moriceau, Small-wavelength geoid and topography anomalies in the South Atlantic Ocean: A clue to new hot-spot tracks and lithospheric deformation, Geophys. Res. Lett. 16 (1989) 637–640.
[14] R.D. Müller, J.-Y. Royer, L.A. Lawver, Revised plate motions relative to the hotspots from combined Atlantic and Indian Ocean hotpot tracks, Geology 21 (1993) 275–278.
[15] W.H.F. Smith, D.T. Sandwell, Global seafloor topography from satellite altimetry and ship depth soundings, Science 277 (1997) 4199–4212.
[16] A. Zindler, S. Hart, Chemical geodynamics, Annu. Rev. Earth Planet. Sci. 14 (1986) 493–571.
[17] J.-G. Schilling, Fluxes and excess temperatures of mantle plumes inferred from their interaction with migrating mid-ocean ridges, Nature 352 (1991) 397–403.
[18] K. Burk, J.T. Wilson, Is the African plate stationary, Nature 239 (1972) 387–389.
[19] I. Baker, N.H. Gale, J. Simons, Geochronology of the St. Helena volcanoes, Nature 215 (1967) 1451–1456.
[20] I. Baker, Petrology of the volcanic rocks of Saint Helena Island, South Atlantic, Geol. Soc. Am. Bull. 80 (1969) 1283–1310.
[21] D.J. Chaffey, R.A. Cliff, B.M. Wilson, Characterization of the St. Helena Magma Source, in: A.D. Saunders, M.J. Nory, (Eds.), Magmatism in the Ocean Basins, Geol. Soc. London Spec. Publ. 42 (1989) 257–276.
[22] S.C. Cande, J.L. LaBrecque, W.B. Haxby, Plate kinematics of the South Atlantic: Chron 34 to present, J. Geophys. Res. 93 (1988) 13479–13492.
[23] S.C. Cande, D.V. Kent, A new geomagnetic time scale for the late Cretaceous and Cenozoic, J. Geophys. Res. 97 (1992) 13917–13951.
[24] C.W. Devey and scientific party, Cruise report SO-84: The St. Helena hotspot, 64, Dept. of Geology and Paleontology, Christian-Albrechts Univ., Kiel, 1993.
[25] J.M. O'Connor, P. Stoffers, J.R. Wijbrans, Migration rate of volcanism along the Foundation Chain, SE Pacific, Earth Planet. Sci. Lett. 164 (1998) 41–59.
[26] G. Wefer, H.D. Schulz, F. Schott, H.B. Hirschleber, Atlantik 91-Expedition, 92-2, University of Hamburg, 1991, 288 pp.
[27] G.B. Dalrymple, W.A. Duffield, High precision $^{40}Ar/^{39}Ar$ dating of Oligocene rhyolites from the Mongollon–Datil Volcanic Field, using a continuous laser system, Geophys. Res. Lett. 14 (1988) 462–464.
[28] G. Fauer, Principles of Isotope Geology, 2nd ed., Wiley, New York, 1986.
[29] D. York, Cooling histories from $^{40}Ar/^{39}Ar$ age spectra: Implications for Precambrian plate tectonics, Annu. Rev. Earth Planet. Sci. 12 (1984) 383–409.
[30] I. McDougall, T.M. Harrison, Geochronology and thermochronology by the $^{40}Ar/^{39}Ar$ method, Oxford University Press, Oxford, 1988.
[31] G.B. Dalrymple, M.A. Lanphere, $^{40}Ar/^{39}Ar$ technique of K–Ar dating: A comparison with the conventional technique, Earth Planet. Sci. Lett. 12 (1971) 300–308.
[32] H.D. Young, Statistical Treatment of Experimental Data, 88, McGraw-Hill, New York, 1962, pp. 5101–5112.
[33] D. York, Least-squares fitting of a straight line with correlated errors, Earth Planet. Sci. Lett. 5 (1969) 320–324.
[34] I. Wendt, C. Carl, The statistical distribution of the mean squared weighted deviation, Chem. Geol. 86 (1991) 275–285.
[35] J.M. O'Connor, P. Stoffers, M.O. McWilliams, Time–space mapping of Easter Chain volcanism, Earth Planet. Sci. Lett. 136 (1995) 197–212.
[36] J.R. Wijbrans, M.S. Pringle, A.A.P. Koppers, R. Scheveers, Argon geochronology of small samples using the Vulkaan argon laserprobe, Proc. K. Ned. Akad. Wetensch. 98 (1995) 185–218.
[37] J.M. Brozena, R.S. White, Ridge jumps and propagations in the South Atlantic ocean, Nature 348 (1990) 149–152.
[38] P.G. Silver, R.M. Russo, C. Lithgow-Bertelloni, Coupling of South American and African plate motion and plate deformation, Science 279 (1998) 60–63.
[39] A.P. Le Roex, Geochemistry, mineralogy and magmatic evolution of the basaltic and trachytic lavas from Gough Island, South Atlantic, J. Petrol. 26 (1985) 149–186.
[40] I. McDougall, C.D. Ollier, Potassium argon ages from Tristan da Cunha, South Atlantic, Geol. Mag. 119 (1982) 87–93.
[41] P.R. Renne, J.M. Glenn, S.C. Milner, A.R. Duncan, Age of Etendeka flood volcanism and associated intrusions in southwestern Africa, Geology 24 (1996) 659–662.
[42] T. Sempere, G. Herail, J. Oller, M.G. Bonhomme, Late Oligocene–early Miocene major tectonic crisis and related basins in Bolivia, Geology 18 (1990) 946–949.
[43] R.M. Russo, P.G. Silver, Cordillera formation, mantle dynamics, and the Wilson cycle, Geology 24 (1996) 511–514.
[44] H.-U. Schmincke, P.P.E. Weaver, J.V. Firth, Shipboard Scientific Party, Background, objectives, and principal results of drilling the clastic apron of Gran Canaria (VICAP), Proc. ODP. Init. Rept. 157, Ocean Drilling Program, College Station, TX, 1995.
[45] R.C. Courtney, R.S. White, Anomalous heat flow and geoid across the Cape Verde Rise: evidence for dynamic support from a thermal plume in the mantle, Geophys. J.R. Astr. Soc. 87 (1986) 815–867.
[46] D. Kempe, J.-G. Schilling, Discovery Tablemount basalt:

Petrology and geochemistry, Contrib. Mineral. Petrol. 44 (1974) 101–115.
[47] R.D. Müller, W.R. Roest and, J.-Y. Royer, Asymmetric sea-floor spreading caused by ridge–plume interactions, Nature 396 (1998) 455–459.
[48] D.L. Anderson, Y.-S. Zhang, T. Tanimoto, Plume heads, continental lithosphere, flood basalts and tomography, in: B.C. Storey, T. Alabaster, R.J. Pankhurst (Eds.), Magmatism and the Causes of Continental Break-up, Geol. Soc. Spec. Publ. 68 (1992) 99–124.
[49] M.K. McNutt, D.W. Caress, J. Reynolds, K.A. Jordahl, R.A. Duncan, Failure of plume theory to explain midplate volcanism in the southern Austral Islands, Nature 389 (1997) 479–482.
[50] J. Phipps Morgan, W.J. Morgan, Y.-S. Zhang, W.H.F. Smith, Observational hints for a plume-fed suboceanic asthenosphere and its role in mantle convection, J. Geophys. Res. 100 (1995) 12753–12767.